A Negative Feedback Loop Regulates Integrin Inactivation and Promotes Neutrophil Recruitment to Inflammatory Sites

A Negative Feedback Loop Regulates Integrin Inactivation and Promotes Neutrophil Recruitment to Inflammatory Sites

Barry McCormick[1], Helen E. Craig[2], Julia Y. Chu[1], Leo M. Carlin[3,4], Marta Canel[1], Florian Wollweber[1,9], Matilda Toivakka[1], Melina Michael[1], Anne L. Astier[1,5], Laura Norton[2], Johanna Lilja[6], Jennifer M. Felton[1,10], Takehiko Sasaki[7], Johanna Ivaska[5], Ingeborg Hers[8], Ian Dransfield[1], Adriano G. Rossi[1] and Sonja Vermeren[1]*

Running Title: Integrin inactivation promotes neutrophil recruitment

[1]Centre for Inflammation Research, University of Edinburgh, Edinburgh, UK.
[2]The Babraham Institute, Babraham Research Campus, Cambridge, UK.
[3]Cancer Research UK Beatson Institute, Glasgow, UK.
[4]Institute of Cancer Sciences, University of Glasgow, Glasgow, UK.
[5]Centre de Physiopathologie Toulouse-Purpan, INSERM U1043, CNRS U5282, Toulouse University, Toulouse, France.
[6]Turku Centre for Biotechnology, University of Turku, Turku, Finland.
[7]Department of Pathology and Immunology, Akita University School of Medicine, Akita, Japan.
[8]School of Physiology, Pharmacology and Neuroscience, University of Bristol, Bristol, UK.
[9]Current address: Institute of Biochemistry and Molecular Biology, University of Freiburg, Freiburg, Germany
[10]Current address: Division of Allergy, Cincinnati Children's Hospital Centre, Cincinnati, OH, USA

*To whom correspondence should be addressed: Sonja.Vermeren@ed.ac.uk
Centre for Inflammation Research, Queen's Medical Research Institute,
47 Little France Crescent, Edinburgh EH16 4TJ, U.K. ORCID 0000-0002-8460-0884

Abstract

Neutrophils are abundant circulating leukocytes that are rapidly recruited to sites of inflammation in an integrin-dependent fashion. Contrasting with the well-characterized regulation of integrin activation, mechanisms regulating integrin inactivation remain largely obscure. Using mouse neutrophils, we demonstrate here that the GTPase activating protein ARAP3 is a critical regulator of integrin inactivation; experiments with Chinese hamster ovary cells indicate this is not restricted to neutrophils. Specifically, ARAP3 acts in a negative feedback loop downstream of PI3K to regulate integrin inactivation. Integrin ligation drives the activation of PI3K and of its effectors, including ARAP3, by outside-in signaling. ARAP3 in turn promotes localized integrin inactivation by negative inside-out signaling. This negative feedback loop reduces integrin-mediated PI3K activity, with ARAP3 effectively switching off its own activator, whilst promoting turnover of substrate adhesions. In vitro, ARAP3-deficient neutrophils display defective PIP3 polarization, adhesion turnover and transendothelial migration. In vivo, ARAP3-deficient neutrophils are characterized by a neutrophil-autonomous recruitment defect to sites of inflammation.

Key points.

1. A negative feedback loop, integrin-PI3K-ARAP3-integrin controls integrin inactivation

2. Integrin inactivation promotes neutrophil transendothelial migration and recruitment

Introduction

Neutrophils are abundant leukocytes that are key to the inflammatory response and provide a first line of defense against infections. Upon stimulation, circulating neutrophils leave the blood stream to be recruited to sites of infection or injury, where they phagocytose and kill pathogens, releasing reactive oxygen species and other cytotoxic agents (1, 2). Inappropriately activated neutrophils can make important contributions to host injury.

Integrins are α/β heterodimeric cell surface receptors that bind to extracellular matrix proteins and transmembrane receptors expressed by activated endothelial cells, bridging them to the cytoskeleton (3). In addition to the major β2 leukocyte integrins, neutrophils also express others, including the ubiquitous β1 integrins. Integrin ligation triggers 'outside-in signaling' to initiate intracellular signaling cascades. This is distinct from 'inside out' signaling, which refers to intracellular signaling events that regulate the integrin ligand binding affinity status. Whilst the mechanism of integrin activation is well characterized in leukocytes, the regulation of integrin inactivation remains largely elusive.

As illustrated by leukocyte adhesion deficiencies, rare genetic diseases characterized by lacking, dysfunctional or activation-impaired β2 integrins, integrins are essential for neutrophil recruitment to sites and clearance of infections (4, 5). A large body of work identified how leukocyte integrins are activated in a mechanism that is crucial for neutrophil recruitment to inflamed sites. Proximally, this involves the adapters talin and kindlin-3 that directly bind to integrin cytoplasmic tails, promoting their activation (6, 7), with Rap and its effectors, RAPL, RIAM and Radil acting upstream. Excessive integrin activity has also been shown to interfere

with leukocyte recruitment (8, 9), but mechanisms governing integrin inactivation in this context remain poorly defined.

Class I (agonist-activated) PI3Ks transduce signals through the generation of the lipid second messengers phosphatidylinositol 3,4,5-trisphosphate (PIP3) by phosphorylation of PI(4,5)P2 in the plasma membrane. Four class I PI3K isoforms exist and are expressed by the neutrophil, α, β, γ and δ (10). Class I PI3K isoforms are activated upon receptor ligation by SH2 domain binding to phosphotyrosine motifs in receptors or their adapters (e.g. in integrin outside-in signaling), G protein βγ subunits as well as Ras/Rho family small GTPases. PIP3 causes the recruitment to the plasma membrane and activation of numerous PI3K effector proteins, including several regulators of small GTPases.

ARAP3 is a PI3K and Rap-regulated GTPase activating protein (GAP) for RhoA and Arf6 that was identified as a PIP3 binding protein from pig neutrophils (11, 12). ARAP3 shares its domain structure with ARAP1/2 which differ in their expression profiles and substrate specificities (11, 13-15). We previously showed ARAP3 to regulate adhesion-dependent processes in the neutrophil (16). The data presented here identify that integrin activation triggers a negative feedback loop downstream of PI3K by which ARAP3 promotes integrin inactivation. Despite focusing here on β1 integrins in neutrophils, we demonstrate that this function of ARAP3 is also broadly applicable elsewhere. As well as causing a polarization and chemotaxis defect in vitro, in vivo, ARAP3-deficiency interferes with efficient neutrophil recruitment to sites of inflammation.

Materials and Methods

Unless indicated otherwise, cell culture reagents were from Gibco, cell culture plastics from Corning and all other materials from Sigma. All reagents were of the lowest available endotoxin grade. PI3K inhibitors (Selleckchem) and final concentrations used were; pan-PI3K, wortmannin (50nM); PI3Kα, BYL-719 (0.25μM); PI3Kβ, TGX-221 (40nM); PI3Kδ, IC87114 (1μM).

Inducible Arap3$^{-/-}$ mouse model

To analyze neutrophils in vitro, 10-12 week old sex-matched *Arap3*$^{fl/fl}$ *ERT2Cre*$^{+}$ mice were induced with a single intraperitoneal injection with 200mg/kg tamoxifen or vehicle, with experiments performed 10-12 days after induction as described (16). For in vivo experiments, age and sex matched *Arap3*$^{fl/fl}$ *ERT2Cre*$^{+}$ mice and *Arap3*$^{+/+}$*ERT2Cre*$^{+}$ controls were subjected to 5 successive gavages with emulsion containing 1.5mg tamoxifen, followed by a rest period of 10 days (Fig S3A for an example). For ease of reading, tamoxifen induced *Arap3*$^{fl/fl}$ *ERT2Cre*$^{+}$ mice (or neutrophils) are referred to in the text as ARAP3-deficient and in figures as -/-, whilst vehicle induced *Arap3*$^{fl/fl}$ *ERT2Cre*$^{+}$ and tamoxifen induced *Arap3*$^{+/+}$*ERT2Cre*$^{+}$ controls are referred to as controls and +/+, with explanations provided in figure legends. All mice were housed in a specific pathogen-free small animal barrier unit at the University of Edinburgh. All animal work was approved by the University of Edinburgh Animal Welfare Committee and conducted under the control of the United Kingdom Home Office (PPL 60/4502 and PFFB 42579).

Neutrophil preparations

Bone marrow-derived mouse neutrophils were prepared on a discontinuous percoll gradient as previously described (17), using endotoxin reagents throughout, yielding ~70% purity as

assessed by cytocentrifuge preparations. Unless stated otherwise, experiments were performed in Dulbecco's PBS supplemented with Ca^{2+} and Mg^{2+}, 1g/L glucose and 4mM sodium bicarbonate ('PBS++').

Adhesion-induced neutrophil functions

Tissue culture wells were coated overnight at 4°C with fibronectin as indicated. Surfaces were washed 3 times with PBS, blocked with 10% FBS in PBS, and washed again before addition of pre-warmed neutrophils. *ROS production* was measured indirectly using chemiluminescence produced by 5 x 10^5 neutrophils per well at 37°C with 150μM luminol and 18.75 U/mL HRP in the presence or absence of TNF-α (20ng/ml final concentration) in luminescence grade 96 well plates (Nunc) using a Cytation plate reader (Biotec) essentially as described (16). Where indicated, neutrophils were pre-incubated with inhibitors for 10 minutes at 37°C at the indicated concentrations. Where blocking peptides were employed, neutrophils were plated onto the immobilized stimuli and the competing peptide, such that both were encountered at the same time. Neutrophil adhesion, spreading and degranulation assays were as previously described (REF). For *adhesion to endothelial cells*, bEND5 cells were seeded into 24 wells, allowed to form confluent monolayers for 2 days and stimulated with 5nM TNF-α for 16 hours. After washing and careful aspiration, 100μl HBSS (with Ca^{2+} and Mg^{2+}) containing 1 x 10^5 neutrophils were added and allowed to bind to the stimulated endothelial cells under gentle rocking. After 30 minutes, non-adherent neutrophils were washed away with HBSS (without Ca^{2+} and Mg^{2+}). Adherent neutrophils were fixed with PFA, labelled for GR1 (clone RB6-8C5, Biolegend) and counted in randomly taken frames (Evos imaging system; AMG/Thermo). *Transendothelial migration* towards the indicated concentrations of MIP2 (R&D Systems) for 1 hour in 6.5mm

transwell inserts with 3μm pore polycarbonate membranes (Corning) were performed as described (17). Transmigrated neutrophils were labelled for GR1, and 8 random fields of view were photographed and counted (20x magnification; EVOS imaging system).

ARAP3 knock-down in αIIbβ3-expressing CHO cells

αIIbβ3-expressing CHO cells were transduced with lentiviral shRNAs directed against mouse ARAP3. shRNA sequences (shRNA1, CTCCGGCTGGAAGGTGTATAT and GGAATCCGCAAGAAGTTAAA; shRNA2, GCAGAAGTGTGCGTCTCTAAA and TGTATGAAGAGCCAGTATATG), identified from the Broad Institute RNAi consortium database [https://portals.broadinstitute.org/gpp/public], were used alongside a non-targeting control (NTC; GCGCGATAGCGCTAATAATTT). Oligos were synthesized (Sigma Genosys), cloned into pLKO.1 (18), inserts sequenced, lentiviral particles generated, transduced CHO cell populations selected with puromycin. Samples were analyzed by Western blot using sheep anti ARAP3 antiserum (11) and anti-human CD41 (MAB7616, R&D Systems) with HSP90 (clone 3H3C27, Biolegend) serving as loading control .

CHO cell adhesion and spreading

Trypsinized CHO cells in PBS++ were preincubated with inhibitors or vehicle for 10 minutes at 37°C as indicated prior to being plated for 30 minutes onto glass coverslips that had been coated with 150μg/ml fibrinogen and blocked with 2% fatty-acid-free BSA. Fixed, washed cells were stained with AF568-conjugated phalloidin (Thermo Fisher); random images were acquired at 20x magnification (EVOS imaging system). Prior to measuring cell areas with ImageJ, binary images were thresholded and the watershed feature applied to define single cells.

Direct analysis of integrin activity status

Activated β1 integrin was detected using an activation epitope specific antibody (clone 9EG7; BD Biosciences) with an AF488-conjugated secondary (Invitrogen). Images were acquired with a 63x objective using a Zeiss LSM780 confocal microscope with Zeiss Zen Black software. The corrected total cellular fluorescence (CTCF) was calculated using ImageJ, by selecting regions for each cell, and nearby regions of background, and applying CTCF = integrated density – (area of selected cell x mean fluorescence of background readings).

Neutrophil binding to an AF647-labelled fibronectin fragment was essentially as described (19) using flow cytometry using a 5L LSRFortessa (BD). Analysis was performed using FlowJo software (V10) by gating for singlets, selecting neutrophils based on forward and side scatter profile, and measuring geometric mean fluorescence intensity. Similarly, CHO cell binding to AF594-labelled fibrinogen (ThermoFisher) as well as activated and total αIIbβ3 on trypsinized CHO cells were detected with fluorescently-conjugated antibodies (clones PAC-1, and A2A9.6 respectively; Biolegend) and analyzed by measuring geometric mean fluorescence intensity of singlets.

Indirect analysis of PI3K activity

Neutrophil lysates were subjected to immunoblotting with an phosphospecific anti-PKB Thr308 (clone C25E6, Cell Signaling Technology) essentially as described (17) with Syk used as loading control (clone 5F5, Biolegend).

Analysis of GFP-PH-PKB reporter distribution

Micropipette chemotaxis assays were conducted, and polar plots were derived and overlaid using Anagraph (Simon Andrews, The Babraham Institute) and QuimP software [(20), Garching Innovation] as described (21).

Neutrophil adhesion under laminar flow conditions

Purified neutrophils were preincubated for 10 minutes at 37ºC with PI3K or vehicle as indicated prior to being perfused through flow chamber slides (Ibidi $VI^{0.4}$) that had been coated with recombinant murine (rm) ICAM-1 (15µg/ml), rm P-selectin (10µg/ml; both Biolegend) and rm CXCL1 (10µg/ml; Biotechne) using a syringe pump (Legato 200, KD Scientific) to deliver a constant shear stress of 1 dyne / cm^2 at 37 ºC. Adhesion under flow was recorded with 20x magnification by time lapse imaging (2.5 images / second) for 1 minute at 1, 5, 10 and 15 minutes after starting the flow. This was done using a Leica IRB inverted microscope equipped with temperature controlled, automated stage (Prior), Orca camera (Hamamatsu) and Micromanager image acquisition software (FiJi). Firmly adherent cells were manually counted using ImageJ.

Lipopolysaccharide-induced acute lung inflammation

LPS-induced ALI was performed essentially as described (22). Some mice received 3µg APC-anti CD45 (30-F11, Biolegend) in 100µl sterile PBS intravenously 15 minutes prior to being sacrificed, 4 hours after LPS administration, such that in lung digest samples, neutrophils could be stratified by $CD45^+$ and $CD45^-$ staining, indicating vascular or interstitial cells, respectively. Lungs were slowly perfused through the right ventricle with 10ml saline, and a portion of the right inferior lobe collected for single cell digestion with collagenase (Roche) and subsequent

214 analysis. BAL cells were counted (NucleoCounter, Sartorius). BAL cells and lung digests were
215 labelled with FITC-anti GR1 and APC-anti CD11b (Biolegend) and analyzed by flow cytometry
216 to calculate total neutrophil numbers ($GR1^{high}$, $CD11b^{+}$). For imaging, lungs were perfused with
217 low melting point agarose, allowed to set on ice, dissected and fixed with formaldehyde. Left
218 lungs were precision sliced 300μm thick using a vibratome (Campden Instruments 5100mz),
219 permeabilized, blocked and labelled for PECAM-1 (clone 2H8, Abcam) and S100A9/MRP14
220 (Hycult Biotech) with DAPI counterstaining. Following brief formaldehyde post-fixation, slices
221 were mounted using Mowiol containing 2.5% w/v DABCO in gaskets and analyzed using a
222 confocal laser scanning microscope to produce tile-scanned z-stacks (Zeiss LSM 880 NLO
223 Airyscan Fast, using a 20x plan Apo 1.0N.A. water immersion objective, 405, 488 and 561nm
224 cw lasers and acquiring in Airyscan Fast mode). Image analysis was performed using IMARIS
225 software (ver 8 and 9, Bitplane, Oxford Instruments). Endothelial surfaces ($PECAM\text{-}1^{+}$) were
226 rendered to allow identification of airway, interstitital or vascular compartments. Vascular and
227 perivascular neutrophils ($S100A9^{+}$) were counted and normalized to the total volume of the
228 vasculature.
229
230 *Statistical analysis*
231 Where data met the assumptions for parametric tests, two-tailed students' t-test, or 1-way
232 ANOVA with Bonferroni-corrected post hoc comparisons were used. Otherwise, the non-
233 parametric Mann-Whitney rank sum test was used for comparisons. For multiple comparisons,
234 ANOVAs with Bonferroni-corrected post hoc comparisons were used. For kinetic experiments
235 (ROS production) the area under the curve was calculated excluding baseline measures, and

236 comparisons were made using a two-tailed students' t-test. P values < 0.05 were considered
237 statistically significant.

Results

We previously described an embryonically lethal *Arap3* knock-out mouse (23), and a tamoxifen-inducible system for the analysis of ARAP3-deficient neutrophils. Apart from leukocyte-specific β2 integrins neutrophils express many others, including ubiquitous β1 integrins that are involved in interactions with extracellular matrix components such as fibronectin and vitronectin. In keeping with our earlier work we observed enhanced effector functions, including adhesion, spreading, ROS production and degranulation, with ARAP3-deficient neutrophils that had been plated onto fibronectin with co-stimulation by TNF-α (Fig S1A-G), but not upon stimulation with formylated peptides (16). This implies that ARAP3 is an important regulator of neutrophil functions downstream of β1 integrin ligation.

ARAP3 promotes neutrophil β1 integrin inactivation

To ascertain whether the hyper-stimulatory effect of fibronectin binding on ARAP3-deficient neutrophils was due to integrin activity, we made use of a blocking peptide, GRGDSPK, that has been shown to compete with fibronectin binding (24, 25). GRGDSPK, but not a control peptide with disrupted RGD motif, interfered with ROS production induced by plating control and ARAP3-deficient neutrophils onto fibronectin-coated plastic in the presence of TNF-α in a concentration-dependent fashion (Fig 1A).

Increased integrin abundance might explain such increased responses. We did, however, not observe any increased surface integrin expression with ARAP3-deficient neutrophils [Fig S1H,J and not shown; (16)]. An alternative explanation would be an activated integrin conformation present in ARAP3-deficient neutrophils. We analyzed binding of suspension control and

ARAP3-deficient neutrophil to a fluorescently tagged soluble fibronectin fragment. In the presence of 1mM Mg^{++}, ARAP3-deficient neutrophils exhibited a significant increase in fibronectin fragment binding compared to controls (Fig 1B,C). We also employed an antibody that binds to an activation epitope present on both human and mouse β1, 9EG7. We plated control and ARAP3-deficient neutrophils onto fibronectin in the presence of TNF-α and observed significantly increased 9EG7 binding with ARAP3-deficiency (Fig 1D,E). We concluded that ARAP3 promotes integrin *inactivation* in the neutrophil.

ARAP3 promotes inactivation of heterologous human αIIbβ3 and endogenous integrins in Chinese hamster ovary cells.

ARAP3 expression is restricted to some myeloid cells and the vasculature in the mouse (not shown), but it is more broadly expressed in epithelial cells in some other organisms (11). To establish whether ARAP3-mediated integrin inactivation is restricted to the neutrophil, we used Chinese hamster ovary (CHO) cells, that had been engineered to express the human platelet integrin αIIbβ3 (26). Taking advantage of the high degree of conservation between hamster and mouse ARAP3 (92% cDNA identity), we generated two ARAP3 knock-down CHO cell populations by expressing distinct pools of mouse ARAP3-targeting shRNAs alongside a population expressing a non-targeting control (NTC) shRNA (Fig 2A).

Surface (but not total) human αIIbβ3 was reduced in both ARAP3 knock-downs (Fig 2A-D). To test whether ARAP3 regulates the activity status of the heterologous αIIbβ3 in CHO cells, we measured binding to fluorescently labelled fibrinogen by suspension CHO cells by flow cytometry. Increased fibrinogen binding was observed with both ARAP3 knock-down

284 populations (Fig 2E, F). Moreover, by employing the activation epitope-specific antibody PAC-
285 1, we noted that the proportion of activated out of total surface αIIbβ3 was increased in ARAP3
286 knock-down cells (Fig 2G), consistent with the notion that ARAP3 regulates inactivation of
287 heterologous human αIIbβ3 integrin in CHO cells, too.
288
289 In cancer cells, increased β1 integrin activity correlates with increased spreading (19). As
290 indirect read-out of integrin activity we therefore also measured the areas occupied by CHO cells
291 that had been plated onto fibrinogen (Fig 2H, J). ARAP3 knock-down CHO cells occupied a
292 significantly larger area than NTC expressing CHO cells, again indicative of ARAP3-dependent
293 control of CHO cell integrins. Preincubating the cells with αIIbβ3 blocking abciximab
294 significantly reduced the area occupied by control and ARAP3 knock-down CHO cells,
295 suggesting that heterologous αIIbβ3 mediated most fibrinogen binding. Interestingly, however,
296 abciximab-preincubated ARAP3 knock-down cells remained more spread than controls,
297 suggesting that ARAP3 inactivates not only αIIbβ3, but also endogenous hamster integrins that
298 were also capable of binding fibrinogen without being affected by the blocking antibody.
299 Inhibiting PI3K significantly reduced the areas occupied by control and ARAP3 knock-down
300 CHO cells. No significant difference remained between experimental groups after treatment with
301 wortmannin. These observations are in keeping with ARAP3 being a PI3K effector that is able to
302 regulate many integrins, including heterologous human αIIbβ3 in CHO cells.
303
304 ***ARAP3 acts in a negative feedback loop downstream of integrin and PI3K***
305 Having established that ARAP3 mediates integrin inactivation, we turned our attention to
306 upstream signaling. In the neutrophil, ARAP3's master regulator PI3K is activated by integrin

307 outside-in signaling downstream of Src family kinases / Syk (27), with PI3Kβ and δ isoforms
308 implicated in mediating integrin-dependent responses (28).
309
310 To probe the relationship between integrin, PI3K and ARAP3, we analyzed ROS production
311 with neutrophils that had been plated onto fibronectin in the presence or absence of TNFα.
312 Integrin ligation-induced ROS depends on PIP3 generation through class I PI3K, in particular
313 PI3Kβ and δ (28), whilst SHIP1 (29) or ARAP3 (Fig 1) deficiency causes increased adhesion-
314 dependent ROS. Inhibiting individual class IA PI3K isoforms reduced adhesion-induced ROS
315 production observed with control and ARAP3-deficient neutrophils, and abrogated significant
316 differences observed between genotypes (Fig 3A).
317
318 ROS production is dependent on PIP3-activated Rac GEFs, inhibition of which could potentially
319 explain the above result. We therefore also analyzed PI3K-dependency of degranulation with
320 control and ARAP3-deficient neutrophils that been stimulated by being plated onto fibronectin in
321 the presence of absence of TNFα. Inhibiting class IA PI3Ks, also reduced the enhanced
322 degranulation that is characteristic of ARAP3-deficient cells; in particular, following PI3Kδ
323 inhibition no significant difference remained between genotypes (Fig 3B).
324
325 We analyzed adhesion and spreading of control and ARAP3-deficient neutrophils after PI3K
326 inhibition to fibronectin-coated plastic. Inhibiting PI3Kβ/δ did not significantly affect the ability
327 of neutrophils to adhere to fibronectin, in keeping with an earlier report that had analyzed
328 neutrophil adhesion to immobilized immune complexes [(28) and not shown]. However, it

resulted in compromised neutrophil spreading in both genotypes, putting an end to significant differences between them (Fig 3C).

Finally, we compared adhesion of neutrophils under constant flow in parallel-plate flow chambers. As previously reported (16), we noted increased neutrophil adhesion with ARAP3-deficient neutrophils compared to controls. Preincubating the neutrophils with a PI3Kβ-specific inhibitor caused decreased neutrophil adhesion in both genotypes (Fig 3D). Notably, this abolished the significant difference in adhesion observed between genotypes in the absence of inhibitor treatment. Together these results show that ARAP3 acts downstream of PI3K in neutrophil adhesion and adhesion-dependent neutrophils functions. Given the heightened responses observed with ARAP3-deficient neutrophils, they also suggest the existence of a negative feedback loop.

For experimental evidence of this feedback loop, we analyzed PKB/Akt Thr308 phosphorylation as an indirect read-out for PI3K activity with neutrophils that did or did not express ARAP3. PKB Thr308 phosphorylation was increased more dramatically in ARAP3-deficient than control neutrophils that had been plated onto the synthetic integrin ligand polyRGD (Fig 3E, F). In contrast, ARAP3-deficiency did not confer increased PKB Thr308 phosphorylation in neutrophils that had been stimulated with the soluble agonist fMLF (Fig 3G, H). We concluded that ARAP3 functions in a negative feed-back loop specifically downstream of integrin-stimulated PI3K to inactivate integrins.

Integrin-PI3K-ARAP3 negative feedback signaling regulates persistent neutrophil polarization during chemotaxis.

Chemotaxing neutrophils are characterized by polarized PIP3 at the pseudopod (30, 31). To analyze whether the negative feedback loop delineated here operates to control neutrophil behavior, we analyzed PIP3 generation in the chemotaxing neutrophil in a spatiotemporal fashion. Having crossed inducible ARAP3 knock-out mice with mice that expressing a PIP3 probe, GFP-PKB-PH (30), we used confocal microscopy to monitor PIP3 production in real-time in control and ARAP3-deficient neutrophils that were allowed to chemotax on glass coverslips towards fMLF. Control cells displayed persistent PIP3 polarization towards the chemoattractant. In contrast, ARAP3-deficient cells were unable to polarize PIP3 persistently, with poles observed to move around cells; more than 50% of ARAP3-deficient neutrophils exhibited additional pole(s) (Fig 4A for an example). We generated polar plots (21, 31), to visualize PIP3 polarization over time in individual neutrophils (not shown). Overlays of these polar plots confirmed the poor persistency of PIP3 polarization of ARAP3-deficient neutrophils (Fig 4B).

In the absence of a probe for activated integrins, we were unable to test whether non-persistent PIP3 polarization of ARAP3-deficient neutrophils coincided with poor turnover of activated integrins. Fixed, adherent fMLP bath-stimulated control and ARAP3-deficient neutrophils were characterized by polarized activated β1 integrin staining at the pseudopod where it coincided with f-actin (Fig S2). For efficient forward motion of the neutrophil, these adhesions must be short-lived. Since ARAP3 is recruited to the plasma membrane by PIP3 (11), it is well placed to

be involved in localized integrin inactivation, ensuring persistence of polarization and directionality.

ARAP3 regulates neutrophil transendothelial migration and recruitment to sites of inflammation.

We next determined the requirement for ARAP3-dependent integrin inactivation in neutrophil recruitment to inflammatory sites. Whereas interstitial migration is thought to be integrin-independent, barriers need to be overcome in an integrin-dependent fashion for neutrophil recruitment, e.g. during transendothelial migration. We first addressed whether the increased integrin activity of ARAP3-deficient neutrophils influences interactions with endothelial cells and transendothelial migration efficiency in vitro. As expected, we found that ARAP3-deficient neutrophils adhered more strongly than controls to monolayers of activated endothelial cells (Fig 5A). Furthermore, ARAP3-deficient neutrophils were characterized by impaired migration to chemoattractant in a model for transendothelial migration, where transwells supported a monolayer of TNFα-stimulated endothelial cells (Fig 5B). In contrast, ARAP3-deficient neutrophils were not defective in transwell chemotaxis (Fig 5C), in line with our previous findings. Together this suggested that ARAP3-dependent integrin inactivation might be relevant for neutrophil recruitment in vivo.

We therefore analyzed neutrophil recruitment in response to LPS-induced acute lung inflammation (ALI) in control and ARAP3-deficient mice. We noted significantly reduced neutrophil numbers in bronchoalveolar lavages from ARAP3-deficient mice compared with

controls (Fig 6A). This held true with bone marrow chimeras, identifying the recruitment defect as neutrophil-autonomous (Fig 6B).

To reach the alveolar space, neutrophils have to breach two barriers, the capillary wall and the alveolar epithelium. To differentiate between neutrophils that were firmly adherent to the luminal side of the vessel wall or undergoing transendothelial migration and those that were interstitial (i.e. that had extravasated but not yet breached the epithelial barrier), we generated precision slices of agarose-perfused, inflamed lung tissue, labelling endothelium and neutrophils. Microscopical analysis of such lung slices suggested that larger numbers of ARAP3-deficient neutrophils had adhered to the lung vasculature and/or were in the process of transmigrating in ARAP3-deficient lungs (Fig 6C, D). We also used flow cytometry for a separate, higher powered quantitative approach to the same question. Mice were administered a fluorescently conjugated anti-CD45 antibody intravenously, labelling fully or partially intravascular leukocytes immediately prior to harvesting PBS-perfused, LPS-inflamed lungs for analysis of tissue homogenates. This identified significantly increased numbers of ARAP3-deficient neutrophils (but not macrophages) which had firmly adhered to the vessel wall or were actively transmigrating at the time of perfusion (Fig 6E; S3B, C). We concluded that ARAP3-mediated neutrophil integrin inactivation enables efficient transendothelial migration, promoting neutrophil recruitment in vivo.

Discussion

The present work identifies ARAP3 as a regulator of integrin *inactivation* in the neutrophil and elsewhere. Our findings place ARAP3 downstream of PI3K in a negative feedback loop that promotes integrin inactivation (Fig 7). This mechanism enables rapid switching off of integrins following ligand binding-induced outside-in signaling. This feedback loop operates in adherent neutrophils, where ARAP3-dependent neutrophil activities are entirely dependent upon outside-in signaling-induced upstream PI3K activity. ARAP3 deficiency results in increased integrin activity, which in turn causes increased integrin-induced PI3K activation and downstream events.

We used integrin-dependent neutrophil chemotaxis as an experimental system in which to analyze the integrin-PI3K-ARAP3-integrin negative feedback loop in a spatiotemporal fashion. ARAP3-deficient neutrophils that chemotaxed on glass towards a point source of chemoattractant polarized PIP3 and generated pseudopods, but these were not persistently directed towards the source of chemoattractant; ARAP3-deficient neutrophils frequently displayed two (or more) poles. This is consistent with the poor integrin-dependent chemotactic migration of these cells (16). In chemotaxis on a 2D matrix, class I PI3Ks are activated downstream of chemoattractant-induced GPCR signaling but also by integrin outside-in signaling. Our results suggest that ARAP3 signaling is engaged to regulate integrin inactivation in response to integrin (but not GPCR) stimulation downstream of PI3K. Our observations are consistent with the possibility that ARAP3 might simply be recruited to PIP3 in the polarized neutrophil to inactivate integrin signaling in a spatiotemporally controlled fashion, limiting further integrin-dependent localized activation of PI3K and enabling pseudopod extension.

Alternatively, further player(s) such as PIP3 metabolizing enzyme(s) might also be recruited to the pseudopod to actively dephosphorylate PIP3. The functions of two PIP3 phosphatases, PTEN and SHIP1, have been analyzed in chemotaxis (29, 30, 32, 33). SHIP1 is activated and functions in adherent neutrophils, where it regulates neutrophil spreading, chemotaxis and PIP3 polarization, whereas PTEN is thought to regulate other features.

Physiologically, interstitial neutrophil migration is thought to be integrin-independent, whereas transendothelial migration is integrin-dependent, with some variability depending on capillary bed and stimulus (1, 2, 34). Our work suggests that in these situations ARAP3-dependent neutrophil integrin inactivation regulates efficient neutrophil recruitment to inflammatory sites by promoting neutrophil extravasation. This identifies that neutrophil extravasation not only requires activation of integrins, but moreover relies on their subsequent *inactivation*. The existence of an integrin inactivation step that regulates efficient immune responses had been predicted by an earlier report, where rendering αLβ2 constitutively active genetically delayed T cell recruitment (9). Similarly, rendering αMβ2 constitutively active using a small molecule interfered with efficient neutrophil recruitment to inflammatory sites (8). Given that ARAP3 is highly expressed in neutrophils, but not in lymphocytes (11), we speculate that integrin inactivation in lymphocytes is controlled by alternative mechanism(s). Given that ARAP1/2 are already implicated in the control of adhesion-dependent processes elsewhere (35, 36), and are expressed in lymphocytes (SV, unpublished), other ARAP family member(s) might be involved.

In addition to demonstrating ARAP3-dependent inactivation of neutrophil β1 integrins, our work shows indirectly that ARAP3 also regulates neutrophil integrins that bind to substrates other than

fibronectin [e.g. vitronectin, fibrinogen, ICAM-1; not shown and (16)]. ARAP3 moreover inactivated heterologous human αIIbβ3 as well as endogenous hamster integrins in CHO cells, again in a PI3K-dependent fashion. Given that ARAP3 is expressed in CHO cells, but not in platelets (which express ARAP2; IH & SV, unpublished), αIIbβ3 is not a likely bona fide ARAP3 'substrate'. Rather, these observations suggest a more general function of ARAP3 downstream of PI3K in integrin inactivation. This is interesting given ARAP3's crucial function in developmental sprouting angiogenesis and lymphangiogenesis (23, 37), processes that are not only absolutely dependent upon integrins (38) but also heavily reliant on chemotaxis, with endothelial cells migrating collectively towards VEGF. It would be interesting to test to which extent the crucial role of ARAP3 downstream of PI3K in sprouting angiogenesis is linked to integrin inactivation.

Integrin inactivation remains incompletely understood. Several scaffold proteins were shown to compete with talin for binding to integrin cytoplasmic tails in what appears to be a cell type-specific fashion. DOK-1 (39, 40) and Filamin-A (41, 42) binding to the β2 cytoplasmic interfered with β2 integrin activation, affecting neutrophil chemotaxis and recruitment. Similarly, SHARPIN binding to β2 in lymphocytes interfered with αLβ2 adopting high affinity or intermediate ligand binding conformations, with its loss reducing adhesion turnover, in vitro migration and delaying homing in vivo (43). Further studies will be required to determine which, if any, of these scaffold proteins are involved in PI3K-ARAP3 mediated integrin inactivation.

Acknowledgements: We thank Len Stephens and Phillip Hawkins (Babraham Institute) for helpful discussions; Simon Walker (Babraham Institute) for help with imaging; Shonna Johnston, Will Ramsay and Mairi Pattison for help with flow cytometry; Simon Andrews (Babraham Institute) and Matthieu Vermeren for bioinformatics; and Ian Handel for help with statistics. We thank Sanford Shattil (UC San Diego) and Robert Weinberg (Whitehead Institute) for providing CHO cells expressing human αIIbβ3 cells and pLKO.1 puro, respectively.

Funding: Work in SV's laboratory was funded by the Medical Research Council UK (MR/K501293/1) and the British Heart Foundation (PG/17/54/32981); a Wellcome Trust Institutional Strategic Support Fund to SV funded the parallel flow chamber work. HEC was supported by BBSRC studentship and MM by a BBSRC-CASE studentship with GSK (BB/R505651/1). AGR and JMF were supported by the Medical Research Council UK (MR/K013386/1). LMC is funded by Cancer Research UK core funding (A23983). Lung slice microscopy was performed in the Beatson Advanced Imaging Resource, supported by Cancer Research UK core funding (A17196). **Author contributions**: Conceptualization – SV, BM, HEC; Data acquisition – BM, HEC, JYC, LC, FW, ALA, MC, MM, JMF, SV; Data analysis – BM, HEC, JYC, ALA, MM, SV; Writing original draft – BM, SV; Writing the revised paper – BM, SV; Funding acquisition – SV, AGR; Resources – MT, JL, JI, ID, IH, TS, LN; Supervision – SV, AGR. All authors approved the final draft. **Competing interests**: The authors declare no competing interests.

Supplementary Materials

This manuscript is accompanied by a data supplement consisting of:

Fig. S1. ARAP3-deficient neutrophils are hyperactive in integrin-dependent situations.

Fig. S2. Activated integrins localize to the leading edge of chemoattractant stimulated neutrophils.

Fig. S3. Deletion of ARAP3 does not affect monocyte/macrophage localization in LPS-ALI.

References

1. Ley, K., C. Laudanna, M. I. Cybulsky, and S. Nourshargh. 2007. Getting to the site of inflammation: the leukocyte adhesion cascade updated. *Nat Rev Immunol* 7: 678-689.
2. Kolaczkowska, E., and P. Kubes. 2013. Neutrophil recruitment and function in health and inflammation. *Nature reviews. Immunology* 13: 159-175.
3. Chu, J. Y., B. McCormick, and S. Vermeren. 2018. Small GTPase-dependent regulation of leukocyte-endothelial interactions in inflammation. *Biochem Soc Trans* 46: 649-658.
4. Svensson, L., K. Howarth, A. McDowall, I. Patzak, R. Evans, S. Ussar, M. Moser, A. Metin, M. Fried, I. Tomlinson, and N. Hogg. 2009. Leukocyte adhesion deficiency-III is caused by mutations in KINDLIN3 affecting integrin activation. *Nat Med* 15: 306-312.
5. Bowen, T. J., H. D. Ochs, L. C. Altman, T. H. Price, D. E. Van Epps, D. L. Brautigan, R. E. Rosin, W. D. Perkins, B. M. Babior, S. J. Klebanoff, and R. J. Wedgwood. 1982. Severe recurrent bacterial infections associated with defective adherence and chemotaxis in two patients with neutrophils deficient in a cell-associated glycoprotein. *J Pediatr* 101: 932-940.
6. Lefort, C. T., J. Rossaint, M. Moser, B. G. Petrich, A. Zarbock, S. J. Monkley, D. R. Critchley, M. H. Ginsberg, R. Fassler, and K. Ley. 2012. Distinct roles for talin-1 and kindlin-3 in LFA-1 extension and affinity regulation. *Blood* 119: 4275-4282.
7. Moser, M., M. Bauer, S. Schmid, R. Ruppert, S. Schmidt, M. Sixt, H. V. Wang, M. Sperandio, and R. Fassler. 2009. Kindlin-3 is required for beta2 integrin-mediated leukocyte adhesion to endothelial cells. *Nat Med* 15: 300-305.
8. Maiguel, D., M. H. Faridi, C. Wei, Y. Kuwano, K. M. Balla, D. Hernandez, C. J. Barth, G. Lugo, M. Donnelly, A. Nayer, L. F. Moita, S. Schurer, D. Traver, P. Ruiz, R. I. Vazquez-Padron, K. Ley, J. Reiser, and V. Gupta. 2011. Small molecule-mediated activation of the integrin CD11b/CD18 reduces inflammatory disease. *Sci Signal* 4: ra57.
9. Semmrich, M., A. Smith, C. Feterowski, S. Beer, B. Engelhardt, D. H. Busch, B. Bartsch, M. Laschinger, N. Hogg, K. Pfeffer, and B. Holzmann. 2005. Importance of integrin LFA-1 deactivation for the generation of immune responses. *J Exp Med* 201: 1987-1998.
10. Hawkins, P. T., and L. R. Stephens. 2015. PI3K signalling in inflammation. *Biochim Biophys Acta* 1851: 882-897.
11. Krugmann, S., K. E. Anderson, S. H. Ridley, N. Risso, A. McGregor, J. Coadwell, K. Davidson, A. Eguinoa, C. D. Ellson, P. Lipp, M. Manifava, N. Ktistakis, G. Painter, J. W. Thuring, M. A. Cooper, Z. Y. Lim, A. B. Holmes, S. K. Dove, R. H. Michell, A. Grewal, A. Nazarian, H. Erdjument-Bromage, P. Tempst, L. R. Stephens, and P. T. Hawkins. 2002. Identification of ARAP3, a novel PI3K effector regulating both Arf and Rho GTPases, by selective capture on phosphoinositide affinity matrices. *Mol Cell* 9: 95-108.
12. Krugmann, S., R. Williams, L. Stephens, and P. T. Hawkins. 2004. ARAP3 is a PI3K- and rap-regulated GAP for RhoA. *Curr Biol* 14: 1380-1384.
13. Miura, K., K. M. Jacques, S. Stauffer, A. Kubosaki, K. Zhu, D. S. Hirsch, J. Resau, Y. Zheng, and P. A. Randazzo. 2002. ARAP1: a point of convergence for Arf and Rho signaling. *Mol Cell* 9: 109-119.
14. Yoon, H. Y., K. Miura, E. J. Cuthbert, K. K. Davis, B. Ahvazi, J. E. Casanova, and P. A. Randazzo. 2006. ARAP2 effects on the actin cytoskeleton are dependent on Arf6-specific GTPase-activating-protein activity and binding to RhoA-GTP. *J Cell Sci* 119: 4650-4666.

15. Craig, H. E., J. Coadwell, H. Guillou, and S. Vermeren. 2010. ARAP3 binding to phosphatidylinositol-(3,4,5)-trisphosphate depends on N-terminal tandem PH domains and adjacent sequences. *Cell Signal* 22: 257-264.
16. Gambardella, L., K. E. Anderson, C. Nussbaum, A. Segonds-Pichon, T. Margarido, L. Norton, T. Ludwig, M. Sperandio, P. T. Hawkins, L. Stephens, and S. Vermeren. 2011. The GTPase-activating protein ARAP3 regulates chemotaxis and adhesion-dependent processes in neutrophils. *Blood* 118: 1087-1098.
17. Vermeren, S., K. Miles, J. Y. Chu, D. Salter, R. Zamoyska, and M. Gray. 2016. PTPN22 Is a Critical Regulator of Fcgamma Receptor-Mediated Neutrophil Activation. *J Immunol*.
18. Moffat, J., D. A. Grueneberg, X. Yang, S. Y. Kim, A. M. Kloepfer, G. Hinkle, B. Piqani, T. M. Eisenhaure, B. Luo, J. K. Grenier, A. E. Carpenter, S. Y. Foo, S. A. Stewart, B. R. Stockwell, N. Hacohen, W. C. Hahn, E. S. Lander, D. M. Sabatini, and D. E. Root. 2006. A lentiviral RNAi library for human and mouse genes applied to an arrayed viral high-content screen. *Cell* 124: 1283-1298.
19. Lilja, J., T. Zacharchenko, M. Georgiadou, G. Jacquemet, N. De Franceschi, E. Peuhu, H. Hamidi, J. Pouwels, V. Martens, F. H. Nia, M. Beifuss, T. Boeckers, H. J. Kreienkamp, I. L. Barsukov, and J. Ivaska. 2017. SHANK proteins limit integrin activation by directly interacting with Rap1 and R-Ras. *Nat Cell Biol* 19: 292-305.
20. Dormann, D., T. Libotte, C. J. Weijer, and T. Bretschneider. 2002. Simultaneous quantification of cell motility and protein-membrane-association using active contours. *Cell Motil Cytoskeleton* 52: 221-230.
21. Norton, L., Y. Lindsay, A. Deladeriere, T. Chessa, H. Guillou, S. Suire, J. Lucocq, S. Walker, S. Andrews, A. Segonds-Pichon, O. Rausch, P. Finan, T. Sasaki, C. J. Du, T. Bretschneider, G. J. Ferguson, P. T. Hawkins, and L. Stephens. 2016. Localizing the lipid products of PI3Kgamma in neutrophils. *Adv Biol Regul* 60: 36-45.
22. Lucas, C. D., D. A. Dorward, M. A. Tait, S. Fox, J. A. Marwick, K. C. Allen, C. T. Robb, N. Hirani, C. Haslett, R. Duffin, and A. G. Rossi. 2014. Downregulation of Mcl-1 has anti-inflammatory pro-resolution effects and enhances bacterial clearance from the lung. *Mucosal immunology* 7: 857-868.
23. Gambardella, L., M. Hemberger, B. Hughes, E. Zudaire, S. Andrews, and S. Vermeren. 2010. PI3K signaling through the dual GTPase-activating protein ARAP3 is essential for developmental angiogenesis. *Sci Signal* 3: ra76.
24. Puech, P. H., A. Taubenberger, F. Ulrich, M. Krieg, D. J. Muller, and C. P. Heisenberg. 2005. Measuring cell adhesion forces of primary gastrulating cells from zebrafish using atomic force microscopy. *J Cell Sci* 118: 4199-4206.
25. Dotterweich, J., R. Ebert, S. Kraus, R. J. Tower, F. Jakob, and N. Schutze. 2014. Mesenchymal stem cell contact promotes CCN1 splicing and transcription in myeloma cells. *Cell Commun Signal* 12: 36.
26. Watanabe, N., L. Bodin, M. Pandey, M. Krause, S. Coughlin, V. A. Boussiotis, M. H. Ginsberg, and S. J. Shattil. 2008. Mechanisms and consequences of agonist-induced talin recruitment to platelet integrin alphaIIbbeta3. *J Cell Biol* 181: 1211-1222.
27. Schymeinsky, J., C. Then, A. Sindrilaru, R. Gerstl, Z. Jakus, V. L. Tybulewicz, K. Scharffetter-Kochanek, and B. Walzog. 2007. Syk-mediated translocation of PI3Kdelta to the leading edge controls lamellipodium formation and migration of leukocytes. *PLoS One* 2: e1132.

28. Kulkarni, S., C. Sitaru, Z. Jakus, K. E. Anderson, G. Damoulakis, K. Davidson, M. Hirose, J. Juss, D. Oxley, T. A. Chessa, F. Ramadani, H. Guillou, A. Segonds-Pichon, A. Fritsch, G. E. Jarvis, K. Okkenhaug, R. Ludwig, D. Zillikens, A. Mocsai, B. Vanhaesebroeck, L. R. Stephens, and P. T. Hawkins. 2011. PI3Kbeta plays a critical role in neutrophil activation by immune complexes. *Sci Signal* 4: ra23.
29. Mondal, S., K. K. Subramanian, J. Sakai, B. Bajrami, and H. R. Luo. 2012. Phosphoinositide lipid phosphatase SHIP1 and PTEN coordinate to regulate cell migration and adhesion. *Mol Biol Cell* 23: 1219-1230.
30. Nishio, M., K. Watanabe, J. Sasaki, C. Taya, S. Takasuga, R. Iizuka, T. Balla, M. Yamazaki, H. Watanabe, R. Itoh, S. Kuroda, Y. Horie, I. Forster, T. W. Mak, H. Yonekawa, J. M. Penninger, Y. Kanaho, A. Suzuki, and T. Sasaki. 2007. Control of cell polarity and motility by the PtdIns(3,4,5)P3 phosphatase SHIP1. *Nat Cell Biol* 9: 36-44.
31. Ferguson, G. J., L. Milne, S. Kulkarni, T. Sasaki, S. Walker, S. Andrews, T. Crabbe, P. Finan, G. Jones, S. Jackson, M. Camps, C. Rommel, M. Wymann, E. Hirsch, P. Hawkins, and L. Stephens. 2007. PI(3)Kgamma has an important context-dependent role in neutrophil chemokinesis. *Nat Cell Biol* 9: 86-91.
32. Heit, B., S. M. Robbins, C. M. Downey, Z. Guan, P. Colarusso, B. J. Miller, F. R. Jirik, and P. Kubes. 2008. PTEN functions to 'prioritize' chemotactic cues and prevent 'distraction' in migrating neutrophils. *Nat Immunol* 9: 743-752.
33. Subramanian, K. K., Y. Jia, D. Zhu, B. T. Simms, H. Jo, H. Hattori, J. You, J. P. Mizgerd, and H. R. Luo. 2007. Tumor suppressor PTEN is a physiologic suppressor of chemoattractant-mediated neutrophil functions. *Blood* 109: 4028-4037.
34. Mizgerd, J. P., H. Kubo, G. J. Kutkoski, S. D. Bhagwan, K. Scharffetter-Kochanek, A. L. Beaudet, and C. M. Doerschuk. 1997. Neutrophil emigration in the skin, lungs, and peritoneum: different requirements for CD11/CD18 revealed by CD18-deficient mice. *The Journal of experimental medicine* 186: 1357-1364.
35. Chen, P. W., R. Luo, X. Jian, and P. A. Randazzo. 2014. The Arf6 GTPase-activating proteins ARAP2 and ACAP1 define distinct endosomal compartments that regulate integrin alpha5beta1 traffic. *J Biol Chem* 289: 30237-30248.
36. Segeletz, S., L. Danglot, T. Galli, and B. Hoflack. 2018. ARAP1 Bridges Actin Dynamics and AP-3-Dependent Membrane Traffic in Bone-Digesting Osteoclasts. *iScience* 6: 199-211.
37. Kartopawiro, J., N. I. Bower, T. Karnezis, J. Kazenwadel, K. L. Betterman, E. Lesieur, K. Koltowska, J. Astin, P. Crosier, S. Vermeren, M. G. Achen, S. A. Stacker, K. A. Smith, N. L. Harvey, M. Francois, and B. M. Hogan. 2014. Arap3 is dysregulated in a mouse model of hypotrichosis-lymphedema-telangiectasia and regulates lymphatic vascular development. *Human molecular genetics* 23: 1286-1297.
38. Avraamides, C. J., B. Garmy-Susini, and J. A. Varner. 2008. Integrins in angiogenesis and lymphangiogenesis. *Nat Rev Cancer* 8: 604-617.
39. Calderwood, D. A., Y. Fujioka, J. M. de Pereda, B. Garcia-Alvarez, T. Nakamoto, B. Margolis, C. J. McGlade, R. C. Liddington, and M. H. Ginsberg. 2003. Integrin beta cytoplasmic domain interactions with phosphotyrosine-binding domains: a structural prototype for diversity in integrin signaling. *Proc Natl Acad Sci U S A* 100: 2272-2277.
40. Gupta, S., J. C. Chit, C. Feng, A. Bhunia, S. M. Tan, and S. Bhattacharjya. 2015. An Alternative Phosphorylation Switch in Integrin beta2 (CD18) Tail for Dok1 Binding. *Sci Rep* 5: 11630.

41. Sharma, C. P., R. M. Ezzell, and M. A. Arnaout. 1995. Direct interaction of filamin (ABP-280) with the beta 2-integrin subunit CD18. *J Immunol* 154: 3461-3470.
42. Sun, C., C. Forster, F. Nakamura, and M. Glogauer. 2013. Filamin-A regulates neutrophil uropod retraction through RhoA during chemotaxis. *PLoS One* 8: e79009.
43. Pouwels, J., N. De Franceschi, P. Rantakari, K. Auvinen, M. Karikoski, E. Mattila, C. Potter, J. P. Sundberg, N. Hogg, C. G. Gahmberg, M. Salmi, and J. Ivaska. 2013. SHARPIN regulates uropod detachment in migrating lymphocytes. *Cell Rep* 5: 619-628.

Figure Legends

Figure 1. ARAP3 promotes β1 integrin inactivation in neutrophils. Neutrophils were prepared from bone marrows of mock (+/+) and tamoxifen induced (-/-) inducible *Arap3* knock-out mice. (A) ROS production was analyzed with neutrophils that had been plated onto 20 μg/ml fibronectin in the presence of absence of 20 ng/ml TNFα together with the indicated concentration of the RGD blocking peptide GRGDSPK or the control peptide GRADSP. Results obtained in 4 separate experiments are combined in this graph. (B, C) Binding of control and ARAP3-deficient neutrophils to a fluorochrome-coupled fibronectin fragment was determined by flow cytometry. A representative experiment (B) and the integrated results from 4 separate experiments (C) are presented. (D, E) Neutrophils were allowed to adhere to fibronectin coated coverslips, fixed and immunostained with a β1 activation epitope-specific antibody. Representative confocal images with corresponding heatmaps of the fluorescence intensity are shown (D); scale bar, 5 μm. (E) Integrated results obtained with 9-18 cells analyzed per genotype from 3 separately performed experiment are plotted. All bar graphs show mean ± SEM; * $P<0.05$; ** $P<0.01$; P-values were calculated by unpaired two-tailed Student's t-tests.

Figure 2. ARAP3 promotes inactivation of heterologous human αIIbβ3 integrin in CHO cells. (A) CHO cells were transduced to express 2 distinct pools of shRNAs directed against mouse ARAP3, or a non-targeting control (NTC). A representative Western blot is shown; HSP90 served as a loading control. (B, C) Surface αIIbβ3 on CHO cell populations was determined by flow cytometry. A representative example (B) and integrated results from 3 separately performed experiments are plotted (C). (D) Integrated results from 3 separately performed Western blots for total cellular αIIbβ3 expression. (E, F) CHO cell binding to fluorescently tagged fibrinogen was analyzed in suspension cultures. A representative example is shown (E) together with results integrated from at least 5 separately performed experiments (F). (G) Activation epitope specific PAC1 staining normalized to the total cell surface αIIbβ3 in each cell population. Integrated results from 3 separately performed experiments are presented. (H, J)

Control and ARAP3 knock-down αIIbβ3 expressing CHO cells that had or had not been preincubated with the αIIbβ3 blocking antibody abciximab or the pan-PI3K inhibitor wortmannin, as indicated, were allowed to adhere to fibrinogen-coated coverslips. Random images were taken and the cell areas analyzed. Results from 4-7 separate experiments are plotted (H) together with representative images (J). Scale bar, 20μm. All bar graphs show mean±SEM. Raw data were analyzed for statistical significance. *P<0.05; ** P<0.01; ***P<0.001. P-values were calculated by 1-way ANOVA with Bonferroni-corrected post-hoc testing (C, D, F, G), and data were analyzed by 2-way ANOVA with Bonferroni post-hoc test, respectively (H). Significant differences between treatments of the same populations are indicated above the individual bars with color-coded symbols (#) whilst difference between NTC control and shRNA expressing cells within each condition are indicated by symbols (*) above brackets.

Figure 3. A negative feedback loop involving integrin, PI3K and ARAP3. Neutrophils were prepared from bone marrows of mock (+/+) and tamoxifen induced (-/-) inducible *Arap3* knock-out mice and (A-D) preincubated with PI3K inhibitors or vehicle controls as indicated. (A) ROS production and (B) gelatinase release were analyzed with neutrophils that had been plated onto 20 μg/ml fibronectin in the presence of absence of 20 ng/ml TNFα. Graphs combine results from 4 separate experiments. (C) Neutrophils were allowed to adhere for 20 minutes to 5μg/ml fibronectin-coated tissue culture plastic in the presence or absence of 20ng/ml TNFα for analysis of spreading. Results obtained in 3 separate experiments are integrated in this graph. (D) Neutrophil adhesion under flow. Neutrophils were perfused at constant shear stress through ICAM1, p-selectin and CXCL1-coated flow chambers as detailed in Materials and Methods. Results obtained in at least 5 separate experiments are combined in the graph shown. (E, F) Neutrophils were allowed to adhere to tissue culture dishes that had been coated with heat inactivated FCS (HI-FCS) or a synthetic pan integrin ligand, polyArgGlyAsp (pRGD) for 15 minutes at 37°C. (G, H) Suspension neutrophils were stimulated with 1μM fMLF for the indicated length of time. Lysates were subjected to SDS-PAGE and Western blots for probing with a phosphospecific Akt/PKB

antibody (Thr308) as well as a loading control (Syk). Representative blots are shown (D, F) and results obtained from 4 separately performed experiments are plotted (E, G). All graphs show mean ± SEM; * $P<0.05$; ** $P<0.01$; (A-C) were analysed by 1-way ANOVA with multiple comparison post-hoc test; (D, H) were analysed by 2-way ANOVA with Bonferroni multiple comparison test. Pairwise comparisons (F) were calculated from raw data by unpaired two-tailed Student's t-tests. (A, F, H) Analyses were performed on the raw data. Symbols in graphs (A-D) refer to differences between control and ARAP3-deficient neutrophils (in the absence of inhibitor treatment). No significant differences between genotypes were identified in (H).

Figure 4. Integrin-PI3K-ARAP3 negative feed-back signaling aids neutrophil polarization. Neutrophils were prepared from bone marrows of mock (+/+) and tamoxifen induced (-/-) inducible *Arap3* knock-out mice expressing a GFP-PKB-PH PIP3 reporter. Cells were allowed to settle on a glass coverslip, and then subjected to a point source of chemoattractant (micropipette). Cells were imaged using a Perkin Elmer spinning disk Nikon Eclipse TE2000E confocal microscope using a 100x oil immersion objective. Images were acquired every second for 5 minutes using a Hamamatsu cooled CCD camera. (A) Stills taken from a representative control and ARAP3-deficient neutrophil. (B) The distribution of the PIP3 probe along the edge of each frame of the movie was analyzed using QuimP software, measuring the image intensity at 100 nodes around the plasma membrane. The signal intensity along the membrane was normalized to that within the cell body. Intensity measurements were plotted using Anagraph, with each frame mapped onto a concentric ring and signal intensity represented by color coding to generate polar plots. The images shown represent overlays of polar plots generated with 25 control, and 24 ARAP3-deficient neutrophils originating from 6 individual animals per genotype.

Figure 5. ARAP3-regulated integrin inactivation promotes transendothelial migration in vitro. Neutrophils were prepared from bone marrows of mock (+/+) and tamoxifen induced (-/-) inducible *Arap3* knock-out mice. Neutrophil adhesion (A) to activated mouse endothelial (bEND5) cells.

Neutrophil transendothelial migration and chemotaxis (B, C) towards the indicated concentrations of chemoattractant in transwells that did (B) or did not (C) support a monolayer of activated bEND5 cells. Graphs integrate data obtained from of 3-4 separate experiments. All bar graphs show mean±SEM. * P<0.05; ** P<0.01. Pairwise comparisons were analyzed by unpaired two-tailed Student's t-tests.

Figure 6. ARAP3 promotes neutrophil recruitment and transendothelial migration in a model of acute lung injury. Cre was induced by repeat tamoxifen dosing inducible *Arap3* knock-out (-/-) and inducible Cre mice (+/+), or their bone marrow chimeras as indicated. (A, B) ALI was induced in control and ARAP3-deficient mice (A) or their bone marrow chimeras (B) by intracheal administration of LPS. Neutrophil numbers retrieved from bronchoalveolar lavages (BAL) are plotted. (C, D) Agarose-perfused, LPS-inflamed lungs were fixed, precision sliced and endothelium, neutrophils and nuclei labelled. Representative examples of rendered, confocal image stacks are presented (C). Solid arrowheads, alveolar neutrophils; unfilled arrowheads, transendothelial / vascular firmly adherent neutrophils. (D) Images taken from 2 mice/genotype were analyzed and neutrophils that were adhering to the vasculature or actively transmigrating counted. Plotted numbers are normalized to the area of vasculature in the respective images. (E) Mice were intravenously administered fluorescently coupled anti-CD45 prior to lavaging of perfused lungs. Vessel-associated, CD45-labelled neutrophils in lung digests are plotted. (A, B, E) Each symbol representative of one mouse; graphs combine data obtained on at least 2 separate occasions. All bar graphs show mean±SEM. * P<0.05; ** P<0.01. P values were calculated by unpaired two-tailed Student's t-tests.

Figure 7. ARAP3 boosts integrin inactivation in a feed-back loop downstream of PI3K in the neutrophil. Schematic depicting how integrin-mediated outside-in signaling activates PI3K to activate ARAP3, which in turn regulates integrin inactivation by negative inside-out signaling in a negative feed-back loop.

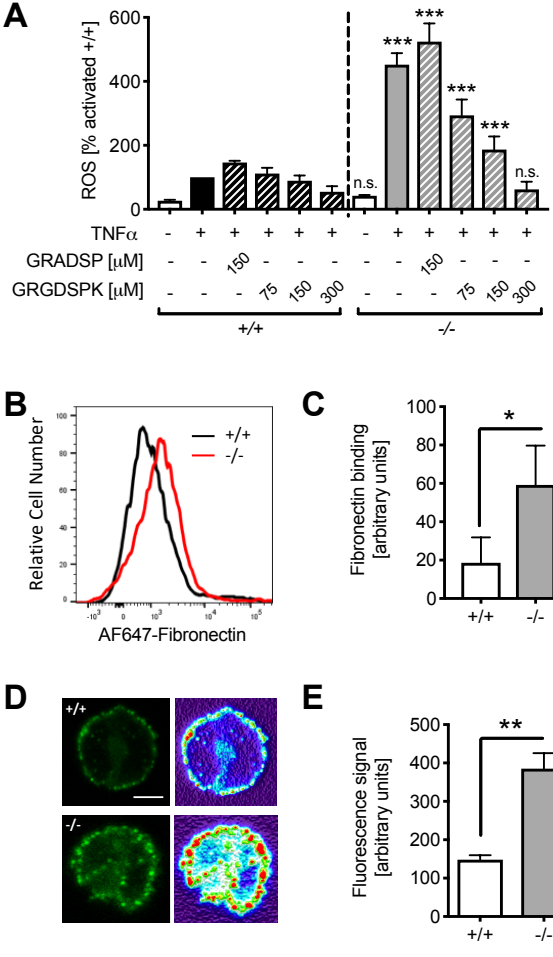

McCormick et al Fig 1

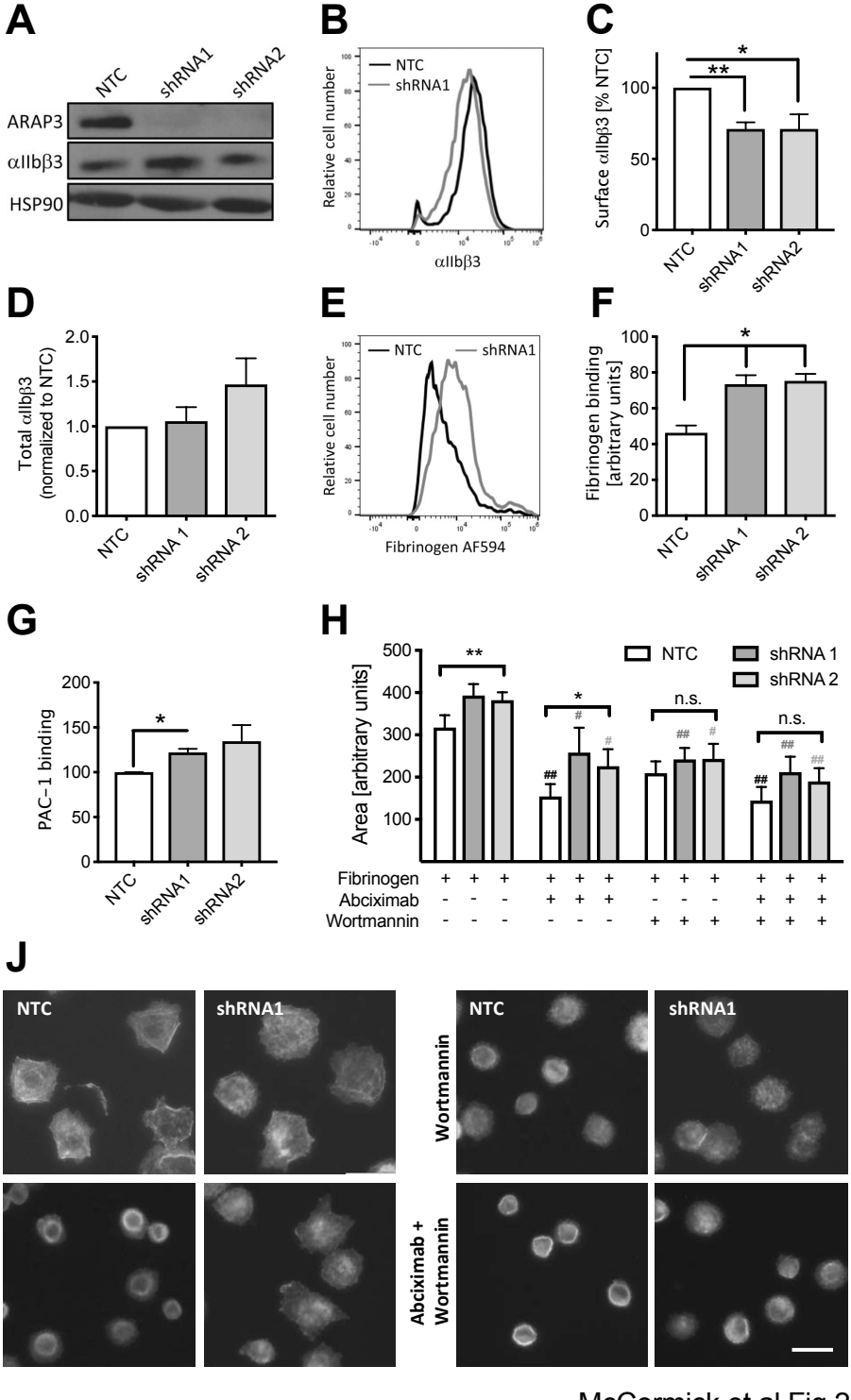

McCormick et al Fig 2

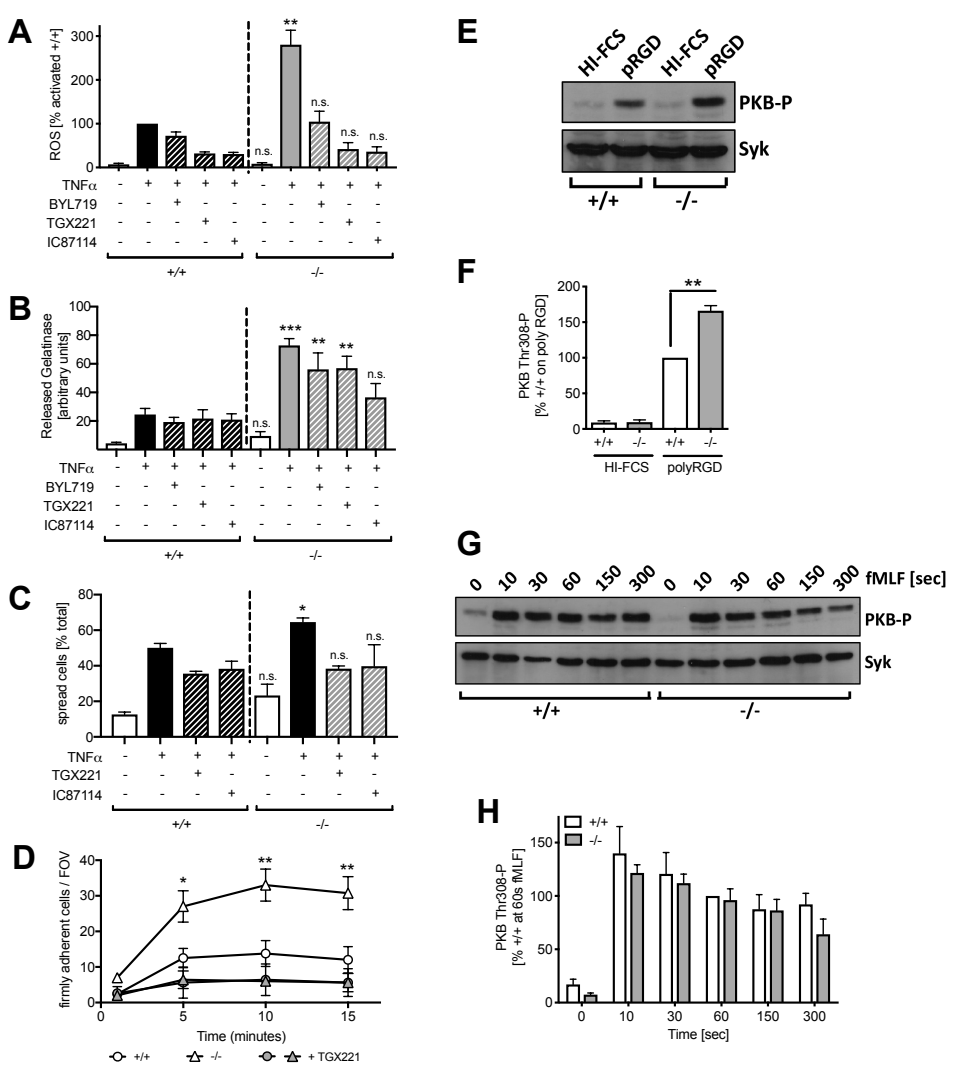

McCormick et al Fig 3

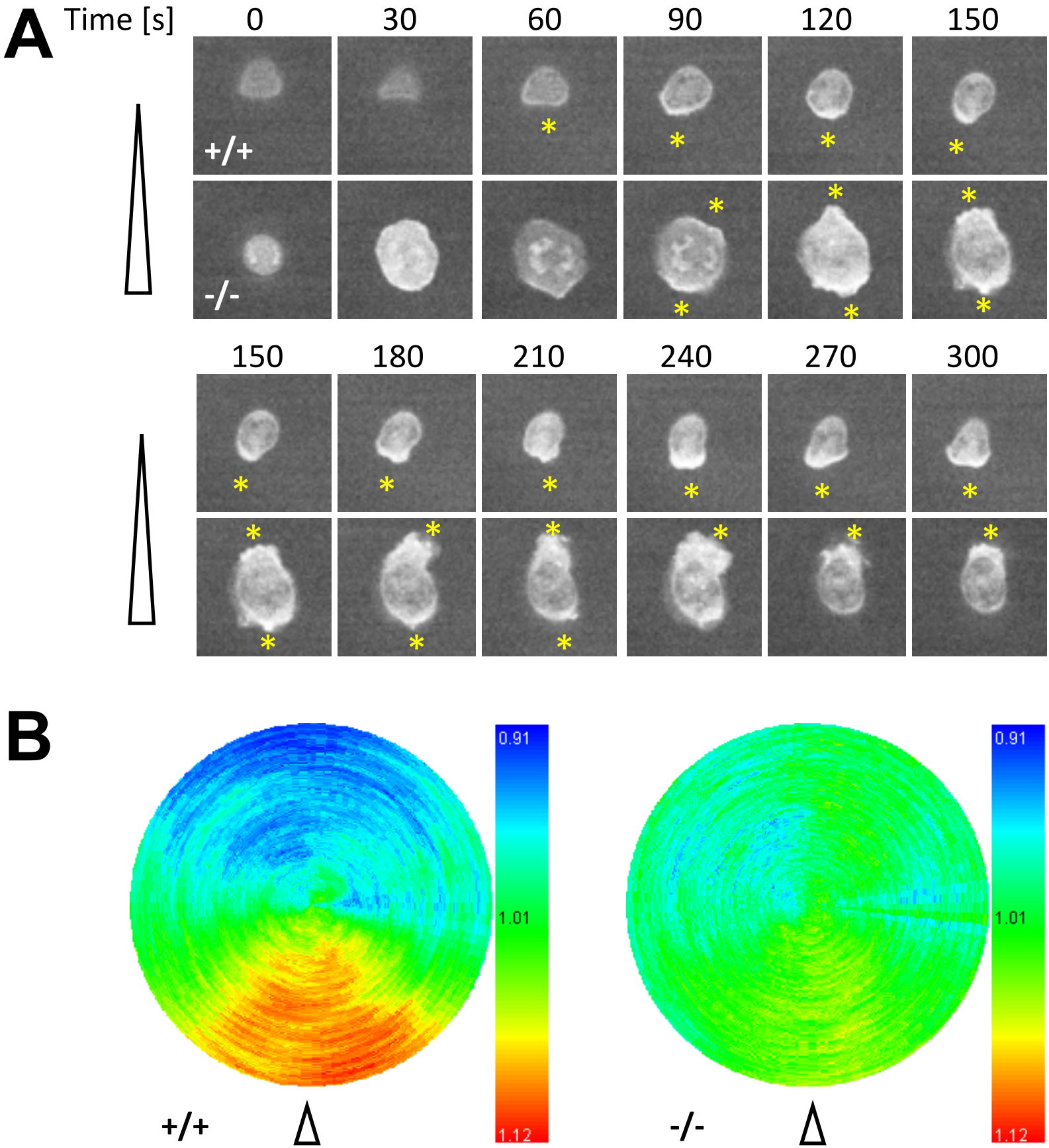

McCormick et al Fig 4

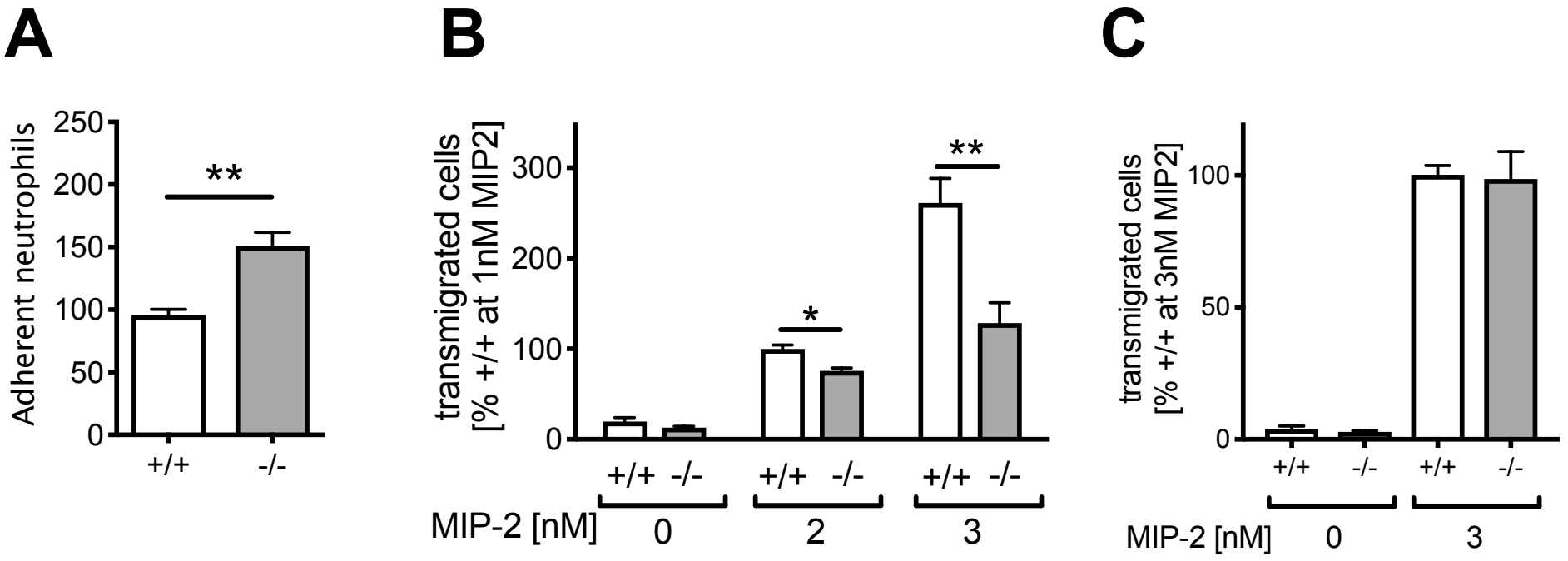

McCormick et al Fig 5

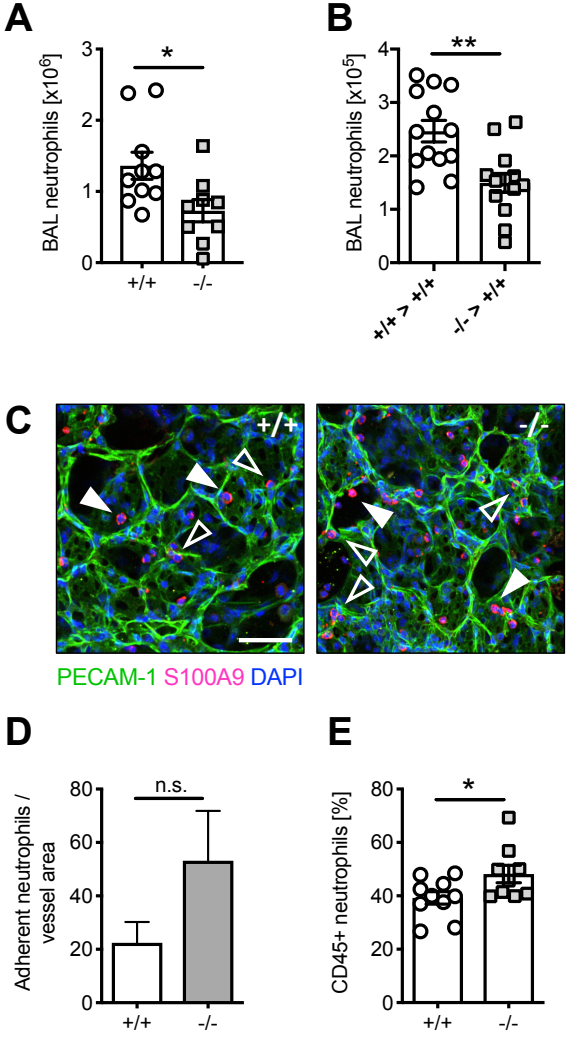

McCormick et al Fig 6

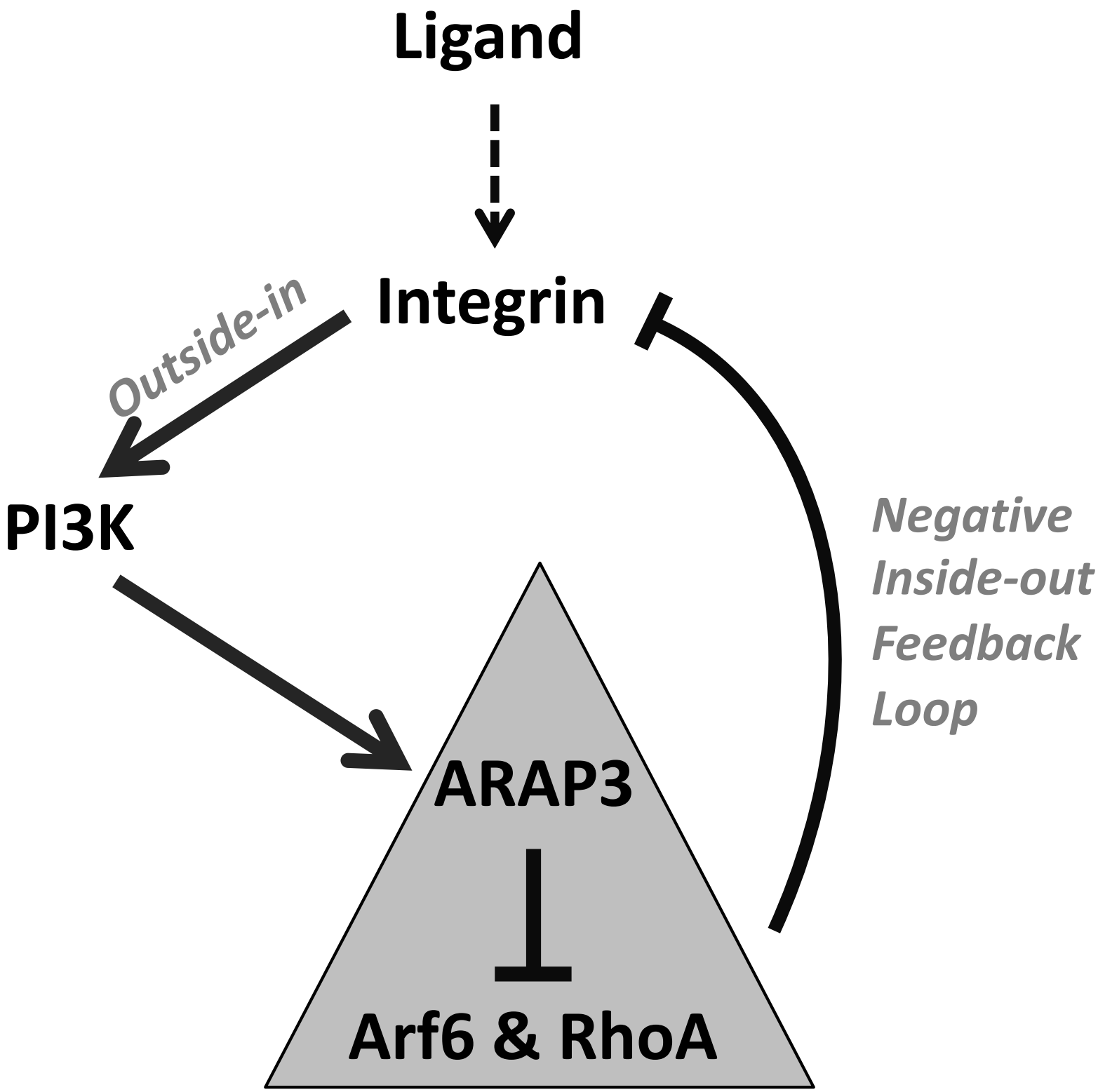

McCormick et al Fig 7